An active vibration control system with decoupling scheme for linear periodically time-varying systems

Junfang Wang[1], Cheuk Ming Mak*[2]

Department of Building Services Engineering, The Hong Kong Polytechnic University, Hung Hom, Kowloon, Hong Kong, China

Abstract

For the active vibration control (AVC) of periodically time-varying (PTV) systems, the filtered-x least mean squares (FXLMS) method is widely applied. Many AVC systems based on FXLMS employ two coupled adaptive processes – online modeling or identification and controller updating – to track the parametric change and realize the real-time updating of the control signal. Errors in one process can affect the other. When one process converges, it takes several steps for the other process to converge. After they both converge, it is difficult to tell whether the controller is optimal or not. Therefore, it is difficult to evaluate the influence of the coupling effect and perform a rigorous derivation. In this study, the new AVC system adopts adaptive identification and nonadaptive control to avoid the coupling effect, and the necessary condition for decoupling is obtained. This condition guarantees that the optimal controller can be obtained the moment the system identification process converges, and meanwhile boosts the convergence of the identification process. The robustness of the identification process with the self-tuning mechanism and the optimization of the controller are proved by rigorous derivation. A simple but representative numerical verification is presented to verify the effectiveness of the proposed AVC system.

[1] E-mail: fangjie726@hotmail.com
[2] E-mail: becmmak@polyu.edu.hk * corresponding author

Key words: Periodically time-varying system, active control, coupling effect, decoupling, H_∞ robustness

1. Introduction

Periodically time-varying (PTV) systems fall into the category of parameter-varying systems whose dynamic parameters change with time or other independent variables (Richards 1983). The phenomenon of varying dynamic parameters can be found in various fields (Richards 1983, Lazarus et al 2010, Elachi 1976, Wang et al 2012, Wang and Mak 2014); for instance, some parameters of unsymmetrical rotating machines vary with time, and the propagation parameters of wave propagation in periodic media vary with distance. This class of structures is governed by differential equations of motion with PTV coefficients, making the systems exhibit remarkable dynamics which is difficult to control. Take linear periodically time-varying (LPTV) systems as an example. According to Claasen and Mecklenbräuker's review (1982), the input-output relation for LPTV systems is $X_{lptv}(f) = \sum_{k=-\infty}^{k=\infty} H_k(f - k/T)F(f - k/T)$. The input-output relation for LPTV systems shows that the input spectrum $F(f)$ has an infinite number of shifted versions $F(f-k/T)$, where T is the period of the parametric variation. Consequently, the output spectrum $X_{lptv}(f)$ is composed of the weighed input spectrum $F(f)$ and its shifted versions at other frequency values. That is to say, an LPTV system is different from a linear time-invariant (LTI) system in which the response at one frequency only comes from the input spectrum at the same frequency: for example, $X_{lti}(f) = H(f)F(f)$. As a result, $X_{lptv}(f)$ is characterized by a series of separate peaks with an interval of $1/T$ at the two sides of one frequency because a peak at that frequency can be moved to other frequencies and create those side peaks at $f-k/T$. This difference can be utilized for active control, such as feedback control incorporating

PTV components (Nielsen and Svensson 1999, Svensson 1995). However, this paper focuses on the active control of PTV systems, and this difference may lead to the invalidity of many active vibration control (AVC) algorithms designed by ignoring the oscillation of time-varying parameters and the resultant side peaks. The situation becomes worse if the systems are nonlinear. Therefore, much research effort has been devoted to the active control of PTV systems (Deng et al 2011, Yanga et al 2004, Zhang et al 2012). Most of the control schemes are dependent on a mathematical or estimated model and cannot converge the moment the model is obtained.

Online modeling is usually required for AVC because of the difficulty of measuring or recovering systematic parameters and the possible inapplicability of some promising methods, i.e. AVC methods without modeling, to a high-order system (Niedzwiecki and Meller 2009 and 2010). The time-varying characteristic of some systematic parameters may require a typical AVC system with a fast online modeling process to catch up on systematic changes and an efficiently updated controller to create destructive vibration. Hence, the filtered-x least mean squares (FXLMS) method (Huang 2012, Zhang et al 2012), characterized by low computational cost and easy implementation, is potentially a competent candidate for the real-time control of time-varying systems. However, it is very difficult to analyze the coupling effects between the two adaptive processes – online modeling and controller updating. On one hand, the performance of one process may negatively influence the other process, leading to accumulated errors, amplified vibration, and destabilized systems (Kim and Swanson 2005). On the other hand, after one process converges, it may take several samples for the other process to converge. This mismatch in terms of the convergence of the two processes makes it hard to tell whether they converge to their optimal values under the present systems situation (Yuan 2006). This coupling effect together with the multi-channel coupling potentially

results in the difficulty to achieve uniform distribution of residual sound fields in multi-input multi-output (MIMO) active control (Fan, Su and Chen 2013).

Given the above disadvantages, in the most recent literature, an active noise control (ANC) system (orthogonal adaptation system) with adaptive system identification and nonadaptive controller design was proposed by Yuan to avoid the coupling effect (Yuan 2006a, b). Although the applicability of this ANC system is limited in time-invariant systems or approximately time-invariant systems, it provided the motivation for this study to propose a control system with adaptive system identification and nonadaptive controller design for PTV systems. Later, Yuan presented a self-learning feedback mechanism, and this mechanism could work as a backup for the orthogonal adaptation system (Yuan 2008). When the stability threat due to modeling errors is detected, the orthogonal adaptation block is switched off and the feedback block is triggered to stabilize and optimize the system without using the estimated model. Nonetheless, this trial-and-error method inevitably leads to slow convergence and may induce the intermittent switch between the two blocks when controlling a time-varying system. Therefore, it would be better if a wide range of dynamic uncertainties and external disturbances could be tuned and tolerated inside one control system, leaving other ones which may not commonly happen to the backup system. In section 3, the range of these disturbances considered in this paper is clarified for the purposes of deriving the identification algorithm and discussing the robustness of the proposed system.

Motivated by Yuan's work, the objective of this paper is to apply this decoupling scheme to the active vibration control of PTV systems. The new AVC system for PTV systems aims at bearing the following characteristics. It consists of one adaptive process for system identification and one nonadaptive process for controller optimization. Besides, the identification process can suppress the

negative influence of dynamic uncertainties and disturbances and exhibit strong robustness to them. The algorithms for both of these processes will be rigorously derived in sections 3 and 4. Simulation results will be presented in section 5 to demonstrate the stability and effectiveness of the new AVC system.

2. Background information and objectives

A typical AVC system can be described by a block diagram (Fig. 1), where H_{po}, H_s, H_r, and H_c are the primary path, secondary path, reference path, and the controller respectively and $\hat{\mathbf{w}}_{po}$ and $\hat{\mathbf{w}}_s$ are finite impulse response (FIR) adaptive estimators of H_{po} and H_s. With the sensor for the reference signal $r(n)$ sufficiently collocated with the primary disturbance $d(n)$, the reference path H_r is a minimum-phase system with a stable inverse. Therefore, Fig. 1(a) is equivalent to Fig. 1(b) since the equivalent primary path $H_p = H_r^{-1} H_{po}$. It is commonly assumed by many researchers that primary and secondary paths can be approximated, with acceptable errors, by FIR filters. This study is based on the same assumption, and so the AVC system resulting from it will be applicable to any PTV systems which satisfy this assumption.

Figure 1

Assuming that the output under control $y(n)$ is governed by the regression model of Eq. (1), the estimated output under control $\hat{y}(n)$ can be expressed by Eq. (2).

$$y(n) = y_p(n) + y_s(n) = \mathbf{w}_p^T(n)\mathbf{r}(n) + \mathbf{w}_s^T(n)\mathbf{u}(n) + v(n) = \mathbf{w}^T(n)\mathbf{X}(n) + v(n) \qquad (1)$$

$$\hat{y}(n) = \hat{y}_p(n) + \hat{y}_s(n) = \hat{\mathbf{w}}_p^T(n)\mathbf{r}(n) + \hat{\mathbf{w}}_s^T(n)\mathbf{u}(n) = \hat{\mathbf{w}}^T(n)\mathbf{X}(n) \qquad (2)$$

In Eqs. (1-2), $\mathbf{w}^T(n) = \left[\mathbf{w}_p^T(n), \mathbf{w}_s^T(n)\right]$ is the optimal estimator with L_p and L_s as their orders and $\hat{\mathbf{w}}^T(n) = \left[\hat{\mathbf{w}}_p^T(n), \hat{\mathbf{w}}_s^T(n)\right]$ is the real-time estimator; $\mathbf{X}^T(n) = \left[\mathbf{r}^T(n), \mathbf{u}^T(n)\right]$ is

the input made up of $\mathbf{r}^T(n) = \left[r(n-L_p+1), \cdots, r(n) \right]$ and $\mathbf{u}^T(n) = \left[u(n-L_s+1), \cdots, u(n) \right]$; and $v(n)$ is an unknown additive disturbance without any assumptions made about its statistical characterization. $\xi(n) = \left(\mathbf{w}(n) - \hat{\mathbf{w}}(n) \right)^T \mathbf{X}(n)$ and $e(n) = \xi(n) + v(n)$ are called the undisturbed identification error and the disturbed identification error. Therefore, the objective of controller design process is to minimize

$$J_c = \left\| \mathbf{w}^T(n) \mathbf{X}(n) \right\|^2,$$

and the objective of system identification process is to drive $\hat{\mathbf{w}}(n)$ to converge to $\mathbf{w}(n)$, or specifically to minimize the Euclidean norm of model error $\varepsilon(n) = \mathbf{w}(n) - \hat{\mathbf{w}}(n)$

$$J(n) = \left\| \mathbf{w}(n) - \hat{\mathbf{w}}(n) \right\|^2.$$

For simplification of denotation, all of the subscripts in the following text except for p, s, and $f(\cdot)$ denote the variables in the parentheses: for example, $\hat{y}_n$ is $\hat{y}(n)$. $f(\cdot)$ is the function for adjusting the abnormal signal and will be used in the identification algorithm in the next section.

3. System identification

3.1 Derivation of online path modeling algorithm

With the expectation that the updated model $\hat{\mathbf{w}}_{n+1}^T = \left[\hat{\mathbf{w}}_{p,n+1}^T, \hat{\mathbf{w}}_{s,n+1}^T \right]$ is close to the present optimal model $\mathbf{w}_n^T = \left[\mathbf{w}_{p,n}^T, \mathbf{w}_{s,n}^T \right]$ with negligible error, an objective function is constructed as a feasible substitute of $J_n = \left\| \mathbf{w}_n - \hat{\mathbf{w}}_n \right\|^2$,

$$J_n = \left\| \hat{\mathbf{w}}_{n+1} - \hat{\mathbf{w}}_n \right\|^2 + \lambda \left| y_n - f(\hat{\mathbf{w}}_{n+1}^T \mathbf{X}_n) \right|^2. \tag{3}$$

where $\tilde{e}_{f,n} = y_n - f(\hat{\mathbf{w}}_{n+1}^T \mathbf{X}_n) = y_n - \tilde{y}_{f,n}$ is the predicted identification error, $\hat{\varepsilon}_n = \hat{\mathbf{w}}_{n+1} - \hat{\mathbf{w}}_n$ is the approximated model error, and λ is the weight; $f(\cdot)$ may be called a self-tuning function

which aims at preventing $\tilde{e}_n = y_n - \hat{\mathbf{w}}_{n+1}^T \mathbf{X}_n = y_n - \tilde{y}_n$ from exceeding a conservatively preset threshold by adjusting $\hat{\mathbf{w}}_{n+1}^T \mathbf{X}_n$. For a linear system, this function may be a fix value or a time-varying value. For a nonlinear system, this function changes with time nonlinearly to avoid the divergence of the algorithm (see Zhang et al 2012). This paper mainly focuses on the application to linear PTV systems.

The reason for an unacceptable $\tilde{e}_n$ is the additive disturbance ν_n. Since there are no restrictions on or assumptions made about ν_n, the sources of ν_n may cover a wide range of dynamic uncertainties and external sources:

(1) Measurement noise; for example, the noise resulting from imperfect sensors.

(2) Modeling errors; for example, the error due to the use of an FIR filter to approximate an infinite impulse response filter (IIR) system.

(3) Other disturbances imposed by unknown sources.

These factors negatively affect identification performance and destabilize a system, and thus it is necessary to take some measures, such as introducing $f(\cdot)$, to suppress this negative influence. The impact of the self-tuning function $f(\cdot)$ on the robustness of the system estimator will be discussed after the algorithm of the estimator is derived.

To obtain an optimal updated model, the objective function J_n is differentiated with respect to $\hat{\mathbf{w}}_{n+1}$, leading to

$$\hat{\mathbf{w}}_{n+1} = \hat{\mathbf{w}}_n + \lambda \dot{f}_{\tilde{y}_n} \tilde{e}_{f,n} \mathbf{X}_n, \tag{4}$$

where $\dot{f}_{\tilde{y}_n} = \left. \frac{df(z)}{dz} \right|_{z=\tilde{y}_n}$. To solve the unknown weight λ and obtain an explicit expression of Eq. (4), three constraint conditions are introduced based on three practical concerns:

(1) The first concern is to avoid the unacceptable predicted identification error $\tilde{e}_n$. This means that

$\tilde{e}_n$ does not need the adjustment and that the identification errors with and without the adjustment by $f(\cdot)$ are nearly same. In other words, the tuned predicted error $\tilde{e}_{f,n}$ and the original predicted error $\tilde{e}_n$ should approach each other as much as possible.

$$\Delta_1^2 = \left[\left(\tilde{e}_{f,n} \right)^2 - \left(\tilde{e}_n \right)^2 \right]^2 \tag{5}$$

Differentiating Eq. (5) with respect to $\hat{\mathbf{w}}_{n+1}$ and setting the result equal to zero,

$$\tilde{e}_n = \dot{f}_{\tilde{y}_n} \tilde{e}_{f,n} \tag{6}$$

is obtained, where $\dot{f}_{\tilde{y}_n} = \left. \frac{\partial f(z)}{\partial z} \right|_{z=\tilde{y}_n}$.

(2) The second concern is to avoid the unacceptable present identification error e_n. This requires that the tuned present error $e_{f,n}$ and the original present error e_n should approach each other as much as possible:

$$\Delta_2^2 = \left[\left(e_{f,n} \right)^2 - \left(e_n \right)^2 \right]^2, \tag{7}$$

where $e_{f,n} = y_n - f(\hat{\mathbf{w}}_n^T \mathbf{X}_n) = y_n - f_{\hat{y}_n}$ is the tuned present error while $e_n = y_n - \hat{\mathbf{w}}_n^T \mathbf{X}_n = y_n - \hat{y}_n$ is the present error. Differentiating Eq. (7) with respect to $\hat{\mathbf{w}}_n$ and setting the result equal to zero,

$$e_n = \dot{f}_{\hat{y}_n} e_{f,n} \tag{8}$$

is obtained, where $\dot{f}_{\hat{y}_n} = \left. \frac{\partial f(z)}{\partial z} \right|_{z=\hat{y}_n}$.

(3) The third concern is fast convergence. To reach a higher convergence rate, the objective is to render Δ_3 negative and minimum by appropriately setting λ.

$$\Delta_3 = \tilde{e}_n^2 - e_n^2 \tag{9}$$

Differentiating Eq. (9) with respect to λ, substituting Eqs. (6) and (8), and setting the result equal to zero,

$$\lambda = \frac{\dot{f}_{\hat{y}_n} e_{f,n}}{\dot{f}_{\tilde{y}_n} \tilde{e}_{f,n} \mathbf{X}_n^T \mathbf{X}_n} \tag{10}$$

is obtained.

Substituting Eq. (10) into Eq. (4), the explicit expression

$$\hat{\mathbf{w}}_{n+1} = \hat{\mathbf{w}}_n + \frac{\dot{f}_{\hat{y}_n} e_{f,n}}{\mathbf{X}_n^T \mathbf{X}_n} \mathbf{X}_n \tag{11}$$

is obtained, which can be slightly modified to

$$\hat{\mathbf{w}}_{n+1} = \hat{\mathbf{w}}_n + \mu \frac{\dot{f}_{\hat{y}_n} e_{f,n}}{\gamma + \mathbf{X}_n^T \mathbf{X}_n} \mathbf{X}_n , \tag{12}$$

where a small positive parameter γ is introduced to avoid the numerical difficulties caused by a small denominator and a positive real scaling factor μ is introduced to control the misadjustment without changing the direction of $\mathbf{X}_n$. From Eq. (12), we can see that this is a noninvasive process because no probing signal is introduced.

3.2 Analysis of robustness by H_∞ criterion (Haykin 1998)

H_∞ norm represents the largest energy gain of a system, and energy gain for an adaptive estimator may be defined as the ratio of the energy due to model error $\left|\xi_{f,n}\right|^2$ or $\left|\xi_n\right|^2$ to the total disturbance energy inputted to the online model $\left|\nu_n\right|^2$ and $\left\|\varepsilon_0\right\|^2$. According to Eq. (1), the present identification error with and without the self-tuning mechanism can be expressed as

$$\left.\begin{aligned} e_{f,n} &= \xi_{f,n} + \nu_n \\ e_n &= \xi_n + \nu_n \end{aligned}\right\}, \tag{13}$$

where $\xi_{f,n} = \mathbf{w}_n^T \mathbf{X}_n - f(\hat{\mathbf{w}}_n^T \mathbf{X}_n)$ is the undisturbed estimation error after the self-tuning adjustment.

To compute the H_∞ norm of the estimator, we proceed as follows. For a periodic time-varying

system with N samples per cycle, the mean-square deviation (MSD) in the k^{th} period is defined as

$$D_{kN} = \frac{1}{N} \sum_{n=kN}^{(k+1)N-1} \left\| \varepsilon_n \right\|^2 . \tag{14}$$

So,

$$D_{kN} - D_{(k+1)N} = \frac{1}{N} \sum_{n=kN}^{(k+1)N-1} \left[\varepsilon_n - \varepsilon_{n+N-1} \right]^T \left[\varepsilon_n + \varepsilon_{n+N-1} \right]. \tag{15}$$

Substituting Eq. (12) into Eq. (15) and neglecting γ, an inequality is obtained in an attempt to bound the energy gain:

$$D_{kN} - D_{(k+1)N} \geq \frac{1}{N} \sum_{n=kN}^{(k+1)N-1} \frac{\mu \dot{f}_{\hat{y}_n}}{\boldsymbol{X}_n^T \boldsymbol{X}_n} \left[(2-\mu) \dot{f}_{\hat{y}_n} \left| \xi_{f,n} \right|^2 - 2(1 - 2\dot{f}_{\hat{y}_n} + \mu \dot{f}_{\hat{y}_n}) \xi_{f,n}^T \nu_n - (2 - 2\dot{f}_{\hat{y}_n} + \mu \dot{f}_{\hat{y}_n}) \left| \nu_n \right|^2 \right] \tag{16}$$

When the condition $0 < \mu \leq 2 - \frac{1}{\dot{f}_{\hat{y}_n}}$ holds, the inequality of Eq. (16) can be recast as

$$D_{kN} - D_{(k+1)N} \geq \frac{1}{N} \sum_{n=kN}^{(k+1)N-1} \frac{\mu \dot{f}_{\hat{y}_n}}{\boldsymbol{X}_n^T \boldsymbol{X}_n} \left[\left| \xi_{f,n} \right|^2 - \left| \nu_n \right|^2 \right]. \tag{17}$$

If the self-tuning mechanism is not triggered, with the consideration of the second constraint in Eq. (7), Eq. (15) becomes

$$D_{kN} - D_{(k+1)N} \geq \frac{1}{N} \sum_{n=kN}^{(k+1)N-1} \frac{\mu}{\boldsymbol{X}_n^T \boldsymbol{X}_n} \left[(2-\mu) \left| \xi_n \right|^2 + 2(1-\mu) \nu_n - \mu \left| \nu_n \right|^2 \right]. \tag{18}$$

When the condition $0 < \mu \leq 1$ is satisfied, the inequality of Eq. (18) is followed by

$$D_{kN} - D_{(k+1)N} \geq \frac{1}{N} \sum_{n=kN}^{(k+1)N-1} \frac{\mu}{\boldsymbol{X}_n^T \boldsymbol{X}_n} \left[\left| \xi_n \right|^2 - \left| \nu_n \right|^2 \right]. \tag{19}$$

Suppose the algorithm runs for $n = (k+1)N$ iterations from $n = 0$ with the initial condition $\hat{\mathbf{w}}(0)$. Letting $\delta = \max(X_n^T X_n)$ and $\delta_f = \max(X_n^T X_n / \dot{f}_{\hat{y}_n})$, starting from $\hat{\mathbf{w}}(0)$ and summing the two sides of the inequalities in Eqs. (17) and (19), the energy gains G_f and G are solved.

$$G_f = \frac{\sum_{n=0}^{(K+1)N-1} \left|\xi_{f,n}\right|^2}{\frac{N\delta_f}{\mu} D(0) + \sum_{n=0}^{(K+1)N-1} \left|\nu_n\right|^2} \le 1 \tag{20a}$$

$$G = \frac{\sum_{n=0}^{(K+1)N-1} \left|\xi_n\right|^2}{\frac{N\delta}{\mu} D(0) + \sum_{n=0}^{(K+1)N-1} \left|\nu_n\right|^2} \le 1 \tag{20b}$$

G_f and G can be rewritten as Eq. (21) by substituting $\rho = D(0) \Big/ \left\|\varepsilon_0\right\|^2$ into Eq. (20):

$$G_f = \frac{\sum_{n=0}^{(K+1)N-1} \left|\xi_{f,n}\right|^2}{\frac{N\delta_f}{\mu} \rho \left\|\varepsilon_0\right\|^2 + \sum_{n=0}^{(K+1)N-1} \left|\nu_n\right|^2} \le 1 \tag{21a}$$

$$G = \frac{\sum_{n=0}^{(K+1)N-1} \left|\xi_n\right|^2}{\frac{N\delta}{\mu} \rho \left\|\varepsilon_0\right\|^2 + \sum_{n=0}^{(K+1)N-1} \left|\nu_n\right|^2} \le 1 \ . \tag{21b}$$

Eqs. (20-21) show that the output energy (the numerator) caused by the identification error never exceeds the total input energy (the denominator) caused by the disturbances consisting of the initial model error ε_0 and the additive disturbance ν.

In the worst case that $\xi(n)$=-$\nu(n)$ and $\xi_f(n)$=-$\nu(n)$, $D(kN) = D(0)$ for all k because $e_n = 0$ and $e_{f,n} = 0$ stop the adaptive algorithm Eq. (12) from updating. G_f and G can arbitrarily approach unity with the increase in N. Therefore, the H_∞ norm of the estimator or the maximum energy gain is unity. Considering the fact that any filter can never have its maximum energy gain limited below unity, the optimal H_∞ norm of any filter can never be less than unity. Therefore, the proposed estimator is H_∞ optimal if $0 < \mu \le 1$ and $\dot{f}_{\hat{y}_n} \ge \frac{1}{2-\mu}$.

3.3 Constructing the self-tuning function $f(\cdot)$

The fundamental requirement for the self-tuning function is that it starts to adjust the estimated output $\hat{y}_n$ when the estimation error exceeds a conservatively preset threshold. So, a preliminary guess may be

$$f(\hat{y}_n) = \alpha \hat{y}_n + (1-\alpha)\begin{cases} \kappa & \hat{y}_n \geq \kappa \\ \hat{y}_n & \hat{y}_n \in (-\kappa, \kappa) \\ -\kappa & \hat{y}_n \leq -\kappa \end{cases}, \tag{22}$$

where $\kappa = |y_n| + \sigma$ is the upper bound of the estimated output and α is an adjustable parameter ($0 \leq \alpha \leq 1$). When $|\hat{y}_n| - |y_n| \geq \sigma$, where σ is threshold, it means the model error $\varepsilon_n = \mathbf{w}_n - \hat{\mathbf{w}}_n$ is unacceptable, and so this self-tuning mechanism is triggered. A signal processing method $h(\cdot)$, like averaging $y_{n-N+1} \cdots y_n$, may be introduced to alleviate the influence of the additive disturbance v. Therefore, κ can be modified as $\kappa = |h(y_n)| + \sigma$. When no signal processing is imposed, $h_{y_n} = y_n$.

As $\dot{f}_{\hat{y}_n} \geq \dfrac{1}{2-\mu}$ is required for the estimator to be H_∞ optimal, $\alpha = \dfrac{1}{2-\mu}$ is set. Eq. (22) does not have a continuous derivative, and so the sigmoid function is chosen to approximate the second term of Eq. (22) because of its similar shape to the second term and the continuity of its derivative. Then, the self-tuning function is modified as

$$f(\hat{y}_n) = \frac{1}{2-\mu}\hat{y}_n + \frac{\beta}{g(\kappa)}\frac{1-e^{-\hat{y}_n g(\kappa)}}{1+e^{-\hat{y}_n g(\kappa)}}. \tag{23}$$

The derivative is

$$\dot{f}_{\hat{y}_n} = \frac{df}{d\hat{y}_n} = \frac{1}{2-\mu} + 2\beta\frac{e^{-\hat{y}_n g(\kappa)}}{(1+e^{-\hat{y}_n g(\kappa)})^2}, \tag{24}$$

where $\beta > 0$ and $g(\kappa) > 0$ are employed to adjust amplitude and threshold. Although they are

related to $(1-\alpha)$, it is unnecessary to know the analytical solution for the relation of $(1-\alpha)$, β, and $g(\kappa)$. This is because the lack of the restriction by the analytical solution creates more flexibility for the configuration of the self-tuning function. After introducing the sigmoid function, the self-tuning function $f_{\hat{y}_n}$ displays the following properties: when $\hat{y}_n = 0$, $f_{\hat{y}_n} = \hat{y}_n$. When $0 < |\hat{y}_n| < |y_n|$ or $0 < |\hat{y}_n| < |h_{y_n}|$, $f_{\hat{y}_n} \approx \hat{y}_n$, with the increase of $|\hat{y}_n|$, the increase in $|f_{\hat{y}_n}|$ becomes slower; the larger $|\hat{y}_n|$ is, the more slowly $|f_{\hat{y}_n}|$ increases. $f_{\hat{y}_n}$ gradually gets close to the shape of the preliminary guess Eq. (22) after $|\hat{y}_n| \geq \kappa$. This is because the second term of $\dot{f}_{\hat{y}_n}$ is the derivative of the sigmoid function and it is monotonically decreasing with the increase in $|\hat{y}_n|$. This property indicates that $\dot{f}_{\hat{y}_n}$ becomes very small when $|\hat{y}_n|$ is unacceptably large, preventing the excessive updating of the path model and a larger model error.

With this self-tuning function, the applicability of this identification algorithm is not only limited to a linear system, but can be extended to some nonlinear systems when the sigmoid function can represent that type of nonlinearity. The reason is listed as follows. In Eq. (23), the first term is a line and it means this one part of this function changes linearly, while the second term is sigmoid function which represents a nonlinear adjustment when the estimation error exceeds the threshold.

4. Controller design

When the identification error $e_{f,n}$ converges, the minimization of y_n requires the minimization of $\hat{y}_n$ since $y_n = e_{f,n} + f(\hat{y}_n)$. Combining $\hat{y}_n = 0$ and $\hat{\mathbf{w}}_n = \hat{\mathbf{w}}_{n+1} - \frac{\dot{f}_{\hat{y}_n} e_{f,n}}{\mathbf{X}_n^T \mathbf{X}_n} \mathbf{X}_n$, we get $y_n = \hat{\mathbf{w}}_{n+1}^T \mathbf{X}_n$. This result is desirable and also expected by the objective function of system identification Eq. (3) so that Eq. (3) can approximate $J_n = \|\mathbf{w}_n - \hat{\mathbf{w}}_n\|^2$ with negligible error. Therefore, any controller which minimizes $\hat{y}_n$ guarantees that Eq. (3) is a reasonable

approximation of $J_n = \left\| \mathbf{w}_n - \hat{\mathbf{w}}_n \right\|^2$. Additionally, by minimizing $\hat{y}_n$, the second term of Eq. (3) can be minimized, which boosts the minimization of Eq. (3) and thus drives the proposed identification algorithm to converge. In other words, by minimizing $\hat{y}_n$, the controller can drive the adaptive algorithm Eq. (12) to converge, and when the modeling process converges, the optimal controller can be obtained simultaneously. Therefore, the convergence of the identification process and the optimization of the controller are synchronized.

One possible controller aiming at minimizing $\hat{y}_n$ is solved by minimizing the practical objective function:

$$J_c(n) = \sum_{k=no}^{n} \left| \hat{y}_k \right|^2 + \lambda_c \left| u_n \right|^2 ,$$

where $no = n-1, n$ and λ_c is the weight of control signal. Because of the special structure of $\mathbf{J}$, $no < n-1$ does not yield a control signal different from the u_n obtained by setting $no = n-1$.

The estimated output $\hat{y}_k$ is formulated by

$$\begin{bmatrix} \hat{\mathbf{y}}_o \\ \hat{y}_n \end{bmatrix} = \left[\mathbf{H}, \mathbf{J} \right] \begin{bmatrix} \mathbf{u}_o \\ u_n \end{bmatrix} + \left[\mathbf{M}, \mathbf{N} \right] \begin{bmatrix} \mathbf{r}_o \\ r_n \end{bmatrix} \tag{25}$$

$$\mathbf{H} = \begin{bmatrix} \hat{\mathbf{w}}_{s,no}^T & & & \\ & \hat{\mathbf{w}}_{s,no+1}^T & & \\ & & \ddots & \\ & & & \hat{\mathbf{w}}_{s,n}^T(1:N-1) \end{bmatrix}, \quad \mathbf{J} = \begin{bmatrix} \mathbf{O}_{(n-no)\times 1} \\ \hat{\mathbf{w}}_{s,n}^T(N) \end{bmatrix}$$

$$\mathbf{M} = \begin{bmatrix} \hat{\mathbf{w}}_{p,no}^T & & & \\ & \hat{\mathbf{w}}_{p,no+1}^T & & \\ & & \ddots & \\ & & & \hat{\mathbf{w}}_{p,n}^T(1:M-1) \end{bmatrix}, \quad \mathbf{N} = \begin{bmatrix} \mathbf{O}_{(n-no)\times 1} \\ \hat{\mathbf{w}}_{p,n}^T(M) \end{bmatrix},$$

where the subscript o indicates old signals. u_n is the optimal control signal to be determined by the past vibration $\hat{\mathbf{y}}_o = \left[y_{no} \cdots y_{n-1} \right]^T$, the past control signal $\mathbf{u}_o = \left[u_{no-L_s+1} \cdots u_{n-1} \right]^T$, and the

past and present reference signals $\mathbf{r}_o = \left[r_{no-L_p+1} \cdots r_{n-1} \right]^T$ and r_n. Differentiating Eq. (25) with respect to u_n and setting the result equal to zero, the optimal control signal u_n is solved.

$$u_n = -\left(\lambda_c + \mathbf{J}^T\mathbf{J}\right)^{-1}\mathbf{J}^T\left(\mathbf{H}\mathbf{u}_p + \mathbf{M}\mathbf{r}_p + \mathbf{N}r_n\right) \tag{26}$$

After the solution of control signal is solved by Eq. (26), the derivation of this AVC system is completed. It is compared with those AVC systems updated by FXLMS method in the following aspects. 1) Those AVC systems are unstable when the phase error during modeling exceeds 90°, while the proposed system possesses H_∞ robustness and the self-tuning function prevents the estimation error from exceeding a preset threshold; 2) FXLMS is an estimation method, and thus the solution of the controller is not necessarily optimal, but the optimal controller of the presented system can be obtained the moment the modeling process converges; 3) due to the coupling effect, after the modeling process converges, it takes several steps for the controller to converge despite its low computational burden at one step; when the controller converges, it's difficult to know if it is optimal. However, the proposed system successfully apply Yuan's decoupling scheme to the vibration control of PTV systems so that the optimal controller can be obtained the moment the modeling process converges. Therefore, the disadvantages of those AVC systems based on FXLMS method are the advantages of the proposed system.

5. Verification and Analysis

From the previous discussion, it is known that the control performance is fundamentally decided by the identification performance because the optimal control signal is solved by one-step calculation after the identification process converges. Thus, if effective control performances under both systematic change (internal change) and excitation change (external change) are

proved, the effectiveness of the identification process and the decoupling scheme are verified. Therefore, the purpose of this numerical verification is to examine the control performance of the proposed AVC system when the controlled system suffers from dynamic uncertainties and external disturbances.

Figure 2

A numerical simulation is conducted on a mass-spring system installed in the center of a simply supported flexible plate (Fig. 2). This system suffers from a periodically time-varying stiffness and an output noise (a shock). Although the system is not complicated, it is very representative since both internal and external uncertainties are involved. This system is governed by Eq. (27), which consists of a canonical PTV equation with damping and the equation of the motion of the plate at the contact point. The external force is $F = \cos(2\pi 70t)$ and the control force is F_c. Assuming the period of stiffness oscillation is 10 seconds, separate peaks with an interval of 0.1Hz at the two sides of $f = 70\text{Hz}$ are excited. The stiffness of the spring varies periodically with an average of $k = (2\pi 70)^2\ \text{N/m}$, a mass weighs $m = 1\text{kg}$, and the damping ratio is $\zeta = 0.01$. ζ is related to damping c by $\zeta = c/2m\Omega$ and $\Omega^2 = k/m$. x_1 is the displacement of the mass, and x_2 the displacement of the center of the plate in time domain. The transfer function at the center of the plate is $Y(s)$, and L in Eq. (27) denotes the Laplace transform. The mobility of the simply supported plate, correspondent to $Y(s)$, is calculated by its physical parameters (Wang and Mak 2013): Young's modulus $\mathrm{E} = 2.1\times10^{10}\ \mathrm{N/m^2}$, density $\rho = 2.8\times10^{3}\ \mathrm{kg/m^3}$, Poisson's Ratio $\nu = 0.2$, and loss factor $\eta = 2\times10^{-2}$. Its dimensions are 3.5m (length) ×3.5m (width) × 0.24m (thickness). Only the first two modes of the plate at about 50Hz and 250 Hz are considered in the calculation of the mobility because of their relatively significant contribution to response of

the mass.

$$\left.\begin{aligned} &\ddot{x}_1 + 2\zeta\left(\dot{x}_1 - \dot{x}_2\right) + k\left(1 - 0.02 * \sin\left(2\pi 0.1t\right)\right)\left(x_1 - x_2\right) = F \\ &x_2 = L^{-1}\left(Y(s)L\left(2\zeta\left(\dot{x}_1 - \dot{x}_2\right) + k\left(1 - 0.02 * \sin\left(2\pi 0.1t\right)\right)\left(x_1 - x_2\right)\right)\right) \end{aligned}\right\} \quad (27)$$

The system is solved by the Matlab/Simulink model and program. Two simulations are conducted for comparison, one simulation employs the proposed AVC system (see Fig. 3) while the other adopts an AVC system with a different identification process adapted by the normalized LMS method (see Fig. 4). Fig. 3 illustrates the contrast between vibration magnitudes with and without control. From Fig. 3(a), it can be seen that significant attenuation of vibration happens after 10 seconds – the oscillation period of the stiffness. Fig. 3(b) displays shows the frequency-domain correspondent of Fig. 3(a). It depicts the effect of the periodically time-varying parameter - the separate peaks with an interval of 0.1Hz at the two sides of $f = 70\text{Hz}$, and thereby highlights the side-peak suppression achieved by the proposed system. Those side peaks do not exist in a time-invariant system and may invalidate the AVC system which is designed based on the commonly used assumption of the time-invariant system.

Figure 3

For comparison, Fig. 4 shows the control performance of the control system with its identification process updated by normalized LMS. Smaller attenuation and more significant oscillation are observed, compared to Fig.3 (a). The better performance in Fig.3 is because the modeling error (identification error) caused by the internal parametric change is limited below the preset threshold by the self-tuning mechanism in the proposed algorithm. Moreover, an impulsive noise with the duration of 0.1 seconds is added to the output at around the 27^{th} second. In this situation, the controlled system experiences both an additive disturbance (external change) and a

variable stiffness (internal change). The convergence after the system encounters this shock is displayed in Fig.5, which demonstrates the stability of the proposed AVC system under the circumstance that the external and internal changes occur simultaneously.

Figure 4

Figure 5

It is not necessary to compare it with a control system with coupling effect. For one thing, if they possess the same identification process, after the identification process converges, the control system with coupling effect spends several extra iterations obtaining the optimal control signal while it takes the presented control system (i.e. the control system with decoupling scheme) only one-step calculation to solve the optimal control signal. So the control system with decoupling scheme possesses obvious superiority in terms of convergence speed. For another thing, if they have different identification processes, it is not realistic and meaningful to tell which system is better because numerous control systems exist. There must be one system better than the proposed system and there must be one system inferior to the proposed system. As different standards exist, like attenuation, convergence speed and control effort, the control system selected for comparison may be superior according to one standard but inferior according to another standard. Therefore, comparison with control systems with coupling effect is a cumbersome and unnecessary task.

6. Discussion of the advantages of the system according to the theoretical development

It is an AVC system designed to suppress periodically time-varying vibration, and it utilizes a decoupling scheme which is characterized by an adaptive process for system identification and a nonadaptive process for controller optimization to avoid the coupling effect. The necessary

condition for the decoupling is presented in Section 4. With the decoupling scheme and the decoupling condition inside the scheme, the two processes can reach synchronous convergence by positively affecting each other. The controller can drive the identification process to converge as long as the controller is optimized by minimizing the output of the estimated model. When the modeling process converges, the controller can be optimized instantly. Therefore, the convergence of system identification and the optimization of the controller are synchronized. In other words, this advantage of the presented AVC system is the disadvantage of those systems with the coupling effect. Moreover, for the system suffering periodically time-varying parameters, the H_∞ robustness is guaranteed by the condition that the derivative of the self-tuning function is no less than $1/(2-\mu)$ where μ is the adjustable parameter. Its implications are twofold. One implication is that the identified model is the H_∞ optimal approximation of the real system once the process of identification converges. The other is that this AVC system has strong robustness to dynamic uncertainties and disturbances when the condition is satisfied.

7. Conclusion

An AVC system with decoupling scheme is proposed to overcome the disadvantages induced by the coupling effect between two adaptive processes in many AVC systems. Numerical verification is performed on a simple but representative system to examine the control performance and stability of the proposed AVC method. The controlled system suffers from an internal dynamic uncertainty that is the periodically time-varying parameter. Significant attenuation of vibration is observed despite the side-peak effect caused by the periodically time-varying stiffness. Besides, it is compared with a control system which is different from the presented system in terms of the

identification algorithm. This comparison proves the AVC system's superior capability of suppressing the modeling error caused by periodically time-varying effect of the systematic parameter. The proposed system has not been compared with a control system with the coupling effect, but the reasons are justified. Moreover, the final numerical simulation examines the response of controlled system under the circumstance of stiffness oscillation and additive impact. It demonstrates the robustness and stability of the proposed system to parametric oscillation and external disturbances. Despite the representative numerical simulation and rigorous derivation, experimental verification is desirable for the practical application of the presented AVC system. Therefore, future investigation may focus on the design of an experimental system for verification.

8. References

Claasen TACM and Mecklenbräuker WFG (1982) On stationary linear time-varying systems. *IEEE Transactions on Circuits and Systems* 29: 169-184.

Deng F, Rémond D, and Gaudiller L (2011) Self-adaptive modal control for time-varying structures. *Journal of Sound and Vibrati*on 330 (14): 3301-3315.

Elachi C (1976) Wave in active and passive periodic structures: A review. *Proceedings of the IEEE* 64: 1666-1698.

Fan R, Su Z, and Cheng L (2013) Modeling, analysis, and validation of an active T-shaped noise. *Journal of the Acoustical Society of America* 134 (3): 1990-2003.

Haykin S (1998) *Adaptive Filter Theory* (5th ed). New Jersey: Pearson Education, Prentice Hall.

Huang X, Zhang ZY, Zhang ZH, Hua H (2012) Multi-channel active vibration isolation for the control of underwater sound radiation from a stiffened cylindrical structure: a numerical study. *ASME Journal of Vibration and Acoustics* 134(1): 011012.1-011012.12.

Kim BJ and Swanson DC (2005) Linear independence method for system identification/secondary path modeling for active control. *Journal of the Acoustical Society of America* 118(3): 1452-1468.

Lazarus A, Prabel B, and Combescure D (2010) A 3D finite element model for the vibration analysis of asymmetric rotating machines. *Journal of Sound and Vibration* 329 (18):3780-3797.

Niedzwiecki M and Meller M (2009) A new approach to active noise and vibration control–Part I: The known frequency case. *IEEE Transactions on Signal Processing* 57(9): 3373-3386.

Niedzwiecki M and Meller M (2010) A new approach to active noise and vibration control–Part II: The unknown frequency case. *IEEE Transactions on Signal Processing* 57(9): 3387-3398.

Nielsen J L and Svensson PU (1999) Performance of some linear time-varying systems in control of acoustic feedback. *Journal of the Acoustical Society of America* 106(1): 240-254.

Richards JA (1983) *Analysis of periodically time-varying systems*. Berlin, Heidelberg, New York: Spring-Verlag.

Svensson PU (1995) Computer simulations of periodically time-varying filters for acoustic feedback control. *Journal of the Audio Engineering Society* 43:667-677.

Wang J, Mak CM, and Yun Y (2012) A methodology for direct identification of characteristic wave-types in a finite periodic dual-layer structure with transverse connection. *Journal of Vibration and Control* 18(9): 1406-1414.

Wang J and Mak CM (2013) An indicator for the assessment of isolation performance of transient vibration. *Journal of Vibration and Control* 19(16): 2459-2468.

Wang J and Mak CM (2014) Adaptive-passive vibration isolation between nonrigid machines and nonrigid foundations using a dual-beam periodic structure with SMA transverse connection. *Journal of Sound and Vibration* (accepted).

Yanga KJ, Hongb KS, and Matsuno F (2004) Robust adaptive boundary control of an axially moving string under a spatiotemporally varying tension. *Journal of Sound and Vibration* 273 (4-5): 1007-1029.

Yuan J (2006a) Orthogonal adaptation for active noise control. *Journal of the Acoustical Society of*

America 120(1): 204-210.

Yuan J (2006b) Orthogonal adaptation for multichannel feedforward control. *Journal of the Acoustical Society of America* 120(6):3723-3729.

Yuan J (2008) Self-learning active noise control. *Journal of the Acoustical Society of America* 124(4): 2078-2084.

Zhang Z, Rustighi E, Chen Y, and Hua H (2012) Active control of the longitudinal-lateral vibration of a shaft-plate coupled system. *Journal of Vibration and Acoustics* 134: 061002.1-061002.11.

9. Figure Captions

Fig. 1. Block diagram of a typical AVC system: (a) The original system; (b) The equivalent system

Fig. 2. The AVC system

Fig. 3. Control performance of the proposed system: (a) Time domain;(b) Frequency domain

Fig. 4. Control performance of the compared system

Fig. 5. Control performance under the circumstance of stiffness oscillation and external impact

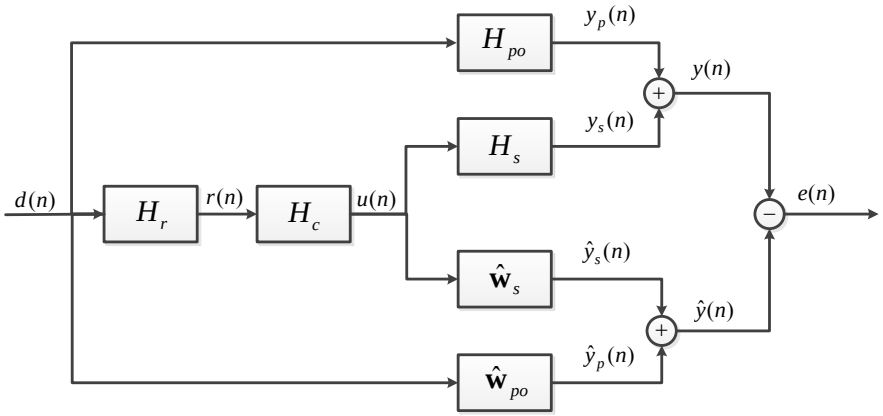

(a)

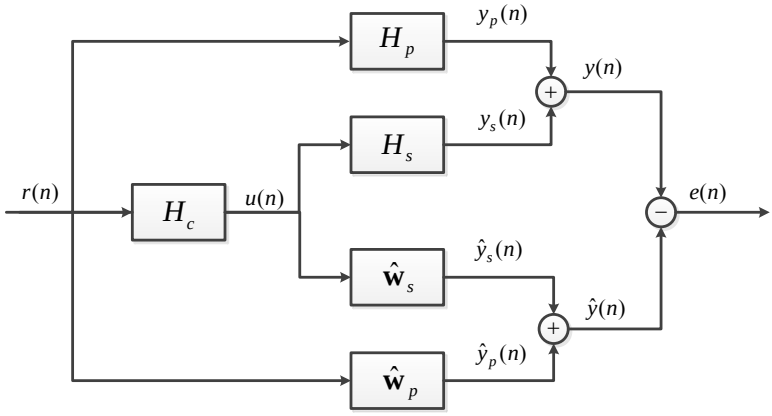

(b)

Fig. 1. Block diagram of a typical AVC system: (a) The original system; (b) The equivalent system

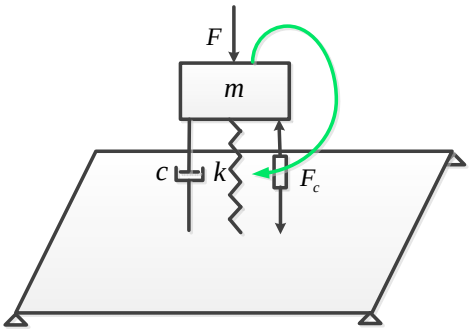

Fig. 2. The AVC system

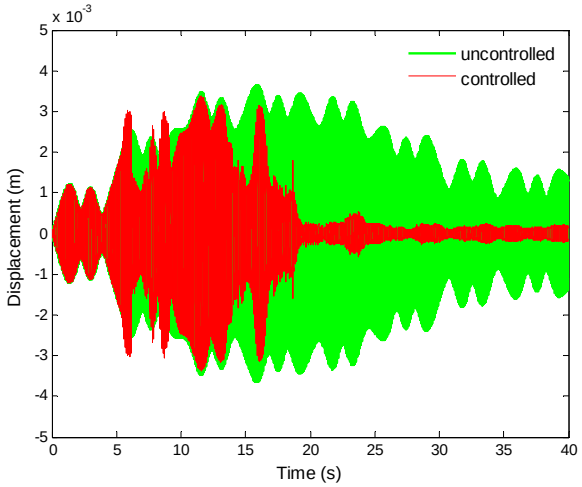

(a)

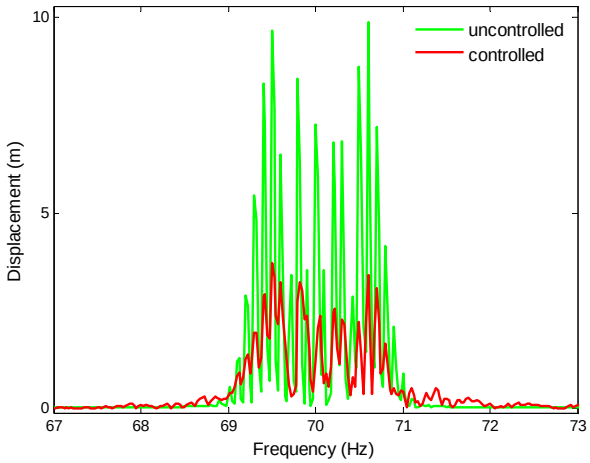

(b)

Fig. 3. Control performance of the proposed system: (a) Time domain;(b) Frequency domain

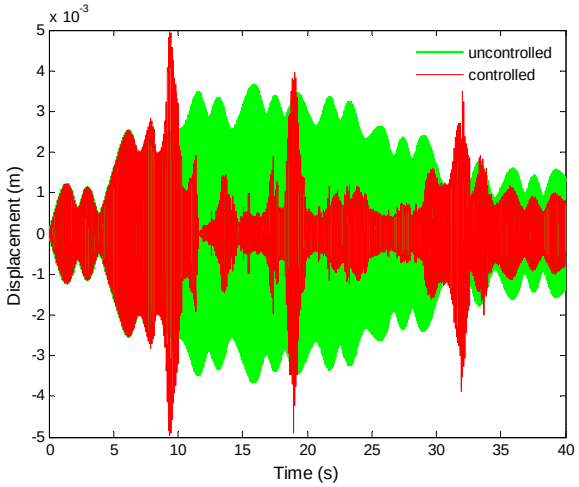

Fig. 4. Control performance of the compared system

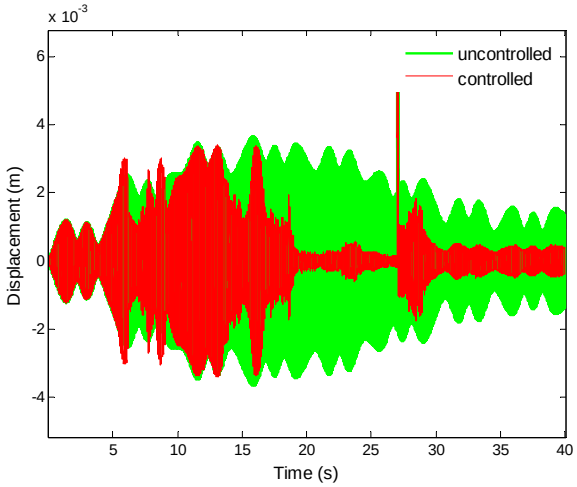

Fig. 5. Control performance under the circumstance of stiffness oscillation and external impact